

# Pressure Recovery Downstream of Disturbances in Closed Conduit Systems

Stephen J. Sanders\*, Michael C. Johnson\*\*

\*(Department of Civil and Environmental Engineering, Utah State University, Logan, Utah USA  
Email: [sanders.stephen17@gmail.com](mailto:sanders.stephen17@gmail.com))

\*\* (Department of Civil and Environmental Engineering, Utah State University, Logan, Utah USA  
Email: [michael.johnson@usu.edu](mailto:michael.johnson@usu.edu))

\*\*\*\*\*

## Abstract:

Pressure recovery in closed conduit systems is essential for optimizing hydraulic efficiency and accurate flow regulation. This study experimentally investigates pressure recovery distances downstream of control valves, flow meters, and orifice plates using a 2-inch stainless steel test bench with pressure taps at 2D intervals up to 26D. Devices tested include orifice plates ( $\beta = 0.3-0.8$ ), a Venturi meter, a butterfly valve, and a gate valve across multiple flow conditions. Results indicate that while industry standards (ANSI/ISA-75.02) recommend measuring pressure at 6D downstream, pressure recovery typically occurs within 4D to 6D, varying based on flow conditions and device geometry. Higher beta ratio orifice plates and Venturi meters exhibited faster recovery, while more restrictive devices, such as partially closed throttling valves, exhibited longer recovery distances. This study also examines the distinction between  $C_v$ -based pressure loss and permanent pressure loss, demonstrating a strong correlation between energy dissipation and the loss coefficient ( $K$ ). These findings provide critical insights into optimizing pressure measurement locations, improving pipeline efficiency, and refining engineering assumptions related to pressure loss assessments in fluid transport systems

**Keywords — Hydraulics, Pressure Measurement, Pressure Recovery, Control Valves, Flow Measurements, Flow Coefficient, Loss Coefficient, Closed Conduit Systems, Permanent Pressure Loss**

\*\*\*\*\*

## I. INTRODUCTION

Pressure recovery plays a critical role in closed conduit systems, particularly downstream of control valves, flow meters, and other fittings. Pressure recovery refers to the process by which the fluid accelerates through a restriction and then decelerates regaining pressure after experiencing disturbances caused by changes in geometry or flow restrictions, such as those introduced by valves and meters. These disturbances create phenomena like flow separation, turbulence, and energy dissipation, which influence where and how quickly pressure stabilizes downstream. Accurate measurement of pressure recovery is essential for optimizing system design and performance, reducing energy losses, and ensuring precise flow regulation.

Control valves, for example, play a vital role in regulating flow and maintaining system performance. They rely on the flow coefficient,  $C_v$  (or  $K_v$ , in SI units), which quantifies a valve’s ability to pass flow at a given pressure drop. The  $C_v$  equation must be used in US customary units, while  $K_v$  is used in SI units. The flow coefficient correlates flow rate to pressure drop at a standard temperature of 60° F (16° C). Each valve’s

flow coefficient varies based on its type, size, and degree of opening, making it integral to predicting pressure drops, head losses, and overall system performance.

The flow coefficient using US customary units,  $C_v$  is calculated using Eq. (1):

$$C_v = \frac{Q}{\sqrt{\frac{\Delta P}{sg}}} \tag{1}$$

Where  $C_v$  is the flow coefficient;  $Q$  is the flow rate in US gallons per minute (gpm);  $\Delta P$  is the differential pressure measured in pounds per square inch (psi); and  $sg$  is the specific gravity of the fluid.

The flow coefficient using SI units,  $K_v$  is calculated using Eq. (2):

$$K_v = Q \sqrt{\frac{sg}{\Delta P}} \tag{2}$$

Where  $K_v$  is the flow coefficient;  $Q$  is the flow rate in cubic meter per hour ( $\text{m}^3/\text{hr}$ );  $\Delta P$  is the differential pressure measured in bars; and  $sg$  is the specific gravity of the fluid.

These equations provide a straightforward method to assess a valve's performance under specific conditions and make comparisons between different flow control valves. However, while  $C_v$  is useful for estimating flow rates, it does not inherently distinguish between pressure losses that are recovered downstream and those that are permanently lost due to turbulence, flow separation, and energy dissipation.

The assumption that pressure fully recovers (excluding permanent losses) downstream of a valve or flow meter can introduce inaccuracies into system design. Many  $C_v$ -based calculations assume that full pressure recovery occurs within a specified distance downstream, but in reality, recovery distances vary depending on the type of valve, flow rate, and system geometry. This variation in recovery behavior can lead to errors in determining actual energy losses and miscalculations of system performance.

The American National Standards Institute (ANSI) and the International Society of Automation (ISA) [1] have established the ANSI/ISA-75.02.01 standard and procedure that is used for flow coefficient testing of control valves. Many manufactures and laboratories use this standard for testing control valves. According to this standard, pressure taps should be placed two nominal pipe diameters upstream and six nominal diameters downstream of the unit under test in regions of uniform, fully developed flow. Figure 1 is an illustration of the installation guidelines given in the ANSI/ISA-75.02.01 standard.

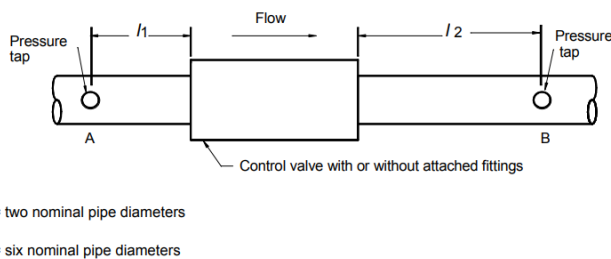


**Figure 1.** Illustration of the ANSI/ISA-75.02.01 standard installation guidelines for control valves, showing the recommended placement of pressure taps 2D upstream and 6D downstream [1].

This configuration is intended to ensure that differential pressure measurements are taken in areas where flow disturbances from the valve have minimal impact, allowing for accurate assessment of the valve's pressure loss and flow coefficient. However, the standard assumes that pressure recovery is complete within six diameters downstream, an assumption that may not hold for all valve types, flow rates, or geometries.

Accurate determination of pressure recovery distances is crucial. If the pressure has not fully recovered by the measurement location, the  $C_v$  or  $K_v$  value calculated for the

valve will be inaccurate, leading to significant errors in system design and operation.

Different valves, meters, and fittings are designed with unique geometries, each creating varying degrees of flow disturbances and pressure recovery behaviors. These factors influence where pressure recovery stabilizes downstream. For example, valves with high flow coefficients or geometries that cause greater turbulence may require longer recovery distances. While prior research has explored some aspects of pressure recovery, gaps remain in understanding how recovery distances vary across devices and flow conditions. This study aims to address these gaps by investigating pressure recovery locations downstream of various valves and meters (a meter or fitting may be considered as a fixed opening valve) over a wide range of flow rates. Additionally, the study evaluates the relationship between  $C_v$ -based pressure loss and permanent pressure loss, quantifying how much pressure is truly recovered versus how much is permanently dissipated due to energy losses.

By addressing these gaps, this research provides critical insights into optimizing flow measurement placement, improving pipeline efficiency, and ensuring accurate system performance predictions.

## II. LITERATURE REVIEW

In *Hydraulics of Pipelines: Pumps, Valves, Cavitation, Transients*, Tullis [2] advises that the placement of pressure taps are important and that the upstream pressure taps can be placed one or more pipe diameter upstream. The downstream pressure taps must be placed so it is beyond the zone of flow establishment. Tullis comments that the point where the pressure recovery is complete varies with the type of valve or minor loss. He suggests that the distance should at least be 5 diameters (D) to 8D downstream.

The International Standard ISO 9644:2008 Agricultural Irrigation Equipment- Pressure Losses in Irrigation Valves- Test Method [3] specifies a testing method for determining the pressure loss in agricultural irrigation valves under steady-state conditions. They specify that pressure taps must be located 2D upstream and 10D downstream of both straight valves and angle or multiport valves. Monserrat [4] used this standard for placing pressure taps when measuring the head loss for a diaphragm valve.

Rahmeyer [5] researched the location that pressure taps should be located to measure differential pressure for butterfly and gate valves sized from 1 in. to 36 in. The tests used pressure taps at 1D and 2D upstream, and at 6D, 8D, and 10D downstream. Test results indicated that only a minimum of 1D upstream, and a minimum of at least 8-10D downstream were needed. Differential pressure measures at 6D downstream were found to be 4% - 8% less than the recovered pressure should have been.

Ball [6] studied pressure distributions, determining the head, and indicating head losses for a 6, 8, 10, and 12-inch gate valves,

and a 6-inch globe valve by placing pressure taps 2D upstream and 12D downstream.

Huang and Kim [7] researched partially open butterfly valves using computational fluid dynamics (CFD) to provide a 3-D numerical flow visualization of incompressible flows around the butterfly valve looking at velocity fields, pressure distributions, streamlines, partial paths, and flow separation. Through trial and error, the authors tested downstream pipe diameters of 3D, 6D, 8D, and 9D to see how long the downstream pipe needs to stabilize flows. The length 3D showed reverse flows at the exit. When 6D was compared to 8D and 9D, the authors noticed that the maximum velocities were different. Comparing 8D and 9D, the maximum velocities were within 2% difference, so the authors concluded that the flows stabilized at 8D downstream and that is what they used throughout their research.

Pradeep [8] studied improving the flow capacity of globe valves by changing their geometry design and using CFD to evaluate how the design change effects the flow capacity. Pressure taps placed at 2D upstream and 6D downstream were used to measure differential pressure for all CFD runs.

Thapa [9] provided an overview of flow measurement and control systems used in the oil and gas industry. Thapa stated that the pressure at the point of recovery for orifice is generally considered to be 8D downstream of the orifice. Thapa suggested using pressure taps located 2.5D upstream and 8D downstream for differential pressure measurement.

Nguyen et al. [10] investigated the pressure distribution and flow coefficient of a 3-inch globe valve by measuring differential pressures at various positions upstream and downstream of the valve. These measurements were compared with the recommendations of the ANSI/ISA-75.01-2012 standard. The study revealed that downstream pressure stabilized within 10D of the valve outlet, indicating that pressure recovery occurs within this range. Additionally, minimal discrepancies in pressure drop calculations were observed when comparing measurement taken 2D to 6D upstream and 6D to 10D downstream of the valve, with differences remaining below 4%.

Notable is that variation exists between various researchers. Consequently, the authors identified the need to address the discrepancies. The intent of this study is to perform laboratory testing on various components to identify where pressure recovers downstream of a disturbance.

### III. THEORETICAL BACKGROUND

In the design of pipelines or water distribution systems, the flow is calculated using the total energy loss in a pipe, derived from Bernoulli's equation, along with any losses that occur due to friction and local disturbances in the system. The energy loss in a pipe or pipe network is the difference in energy between two locations in that pipe or network. The energy change can be expressed as Eq. 3.

$$\frac{P_1}{\gamma} + Z_1 + \frac{V_1^2}{2g} - H_L = \frac{P_2}{\gamma} + Z_2 + \frac{V_2^2}{2g} \quad (3)$$

Where  $P$  = pressure;  $\gamma$  = specific weight;  $Z$  = elevation above the datum;  $V$  = average pipe velocity;  $g$  = acceleration due to gravity;  $H_L$  = total head loss between location 1 and 2. In this equation,  $\frac{P}{\gamma}$  is the pressure head,  $Z$  is the elevation head, and  $\frac{V^2}{2g}$  is the velocity head. The term  $H_L$  represents the energy lost between the two points due to friction and local disturbances. The total head loss can be calculated by summing losses due to friction and the local losses, as shown in Eq.4.

$$H_L = H_f + \sum H_{local} \quad (4)$$

Where  $H_f$  = head loss due to friction;  $H_{local}$  = head loss due to local or minor losses such as valves, fittings, meters, and bends. Substituting the Darcy-Weisbach equation for frictional losses and the minor loss equation for local disturbances, the total head loss equation becomes Eq. 5.

$$H_L = f \frac{L V^2}{D 2g} + \sum K \frac{V^2}{2g} \quad (5)$$

Where  $f$  = Darcy friction factor;  $L$  = pipe length;  $D$  = inside pipe diameter;  $K$  = local loss coefficient; other variables are as previously defined. The first term  $f \frac{L V^2}{D 2g}$  represents the losses due to friction along the length of the pipe, while the second term  $\sum K \frac{V^2}{2g}$  represents the local losses caused by valves, fittings, and other components. Local losses occur due to changes in the flow direction, flow separation, pipe expansions or contractions, and viscous turbulent losses that disrupt the streamlines. Each type of valve or fitting introduces a local disturbance to the flow, which is quantified by as corresponding loss coefficient  $K$ . The total losses are the sum of these individual losses.

For an example, when flow passes through a control valve, the flow is constricted, causing local acceleration and disruption in the streamlines. This results in energy loss due to flow separation, turbulence, and non-uniform velocity in and downstream of the valve. These effects are accounted for using the local loss coefficient  $K$  specific to the valve.

The  $C_v$  or  $K_v$  value of a valve is a standard industry parameter that represents the flow coefficient as previously discussed. The  $C_v$  or  $K_v$  value, which is provided by the manufacturer, indicates the amount of flow the valve can pass with a specified pressure drop across the valve. This value also provides a means to convert the valve's flow characteristics into the corresponding  $K$  loss coefficient. The Crane Technical Paper No. 410 provides an equation to convert  $C_v$  into  $K$  for incompressible fluids as shown in Eq. 6. It's important to note that this procedure can also be done for  $K_v$  values using a different equation.

$$K = \frac{894 * D^4}{C_v^2} \quad (6)$$

Where  $K$  = loss coefficient;  $D$  = inside pipe diameter; and  $C_v$  = valve flow coefficient. This relationship between the loss coefficient and flow coefficient shows that as the  $C_v$  increases (indicating less resistance), the corresponding  $K$  value decreases (indicating lower energy loss through the valve), and vice versa. This connection allows engineers to use  $C_v$  values from valve manufacturers to calculate the local losses in pipeline systems. To better understand the discrepancies between various researchers, laboratory experiments were conducted to quantify pressure recover downstream of several flow disturbances.

#### IV. EXPERIMENTAL PROCEDURE

All the data for this study was collected at the Utah Water Research Laboratory (UWRL) in Logan, Utah. This study was designed to evaluate the pressure recovery locations for various orifice plates, a Venturi meter, a gate valve, and a butterfly valve across a range of flow rates and valve openings when applicable. A test bench utilizing standard 2-inch stainless steel pipe with an inner diameter of 2.067 inches and the aforementioned devices was used for this study. Before assembling the test bench, the friction factor for the stainless steel pipe was determined experimentally. Following this, the pipe was cut, and pressure taps were added.

The test setup included a minimum of 20D of approach pipe, with a pressure tap located 2D from the end of the first section for upstream pressure readings. The downstream section contained 13 pressure taps, spaced at 2D intervals from 2D to 26D downstream. Figure 2 illustrates the configuration of the test section. Each pressure tap was equipped with a shut-off valve, allowing differential pressure measurements between various points along the pipe. All burrs were removed from the pressure taps to ensure accurate differential pressure readings, and each pressure tap was tested to confirm accuracy.



**Figure 2.** Schematic of the experimental test section showing pressure tap locations at 2D intervals downstream (from 2D to 26D). The upstream tap is located at 2D upstream of the test section.

The test section was constructed with flanges at each end to facilitate the installation of a valve or meter between the two pipe test sections, enabling differential pressure measurements using the upstream and downstream taps at a variety of flow rates. Testing was completed in accordance with ANSI/ISA-75.02 standards.

This study examined 2-inch orifice plates with beta ratios ( $\beta$ ) of 0.8, 0.7, 0.6, 0.5, 0.4, and 0.3. The beta ratio is defined as the ratio of the orifice's bore diameter to the inside diameter of the pipe. Figure 3 presents the six 2-inch orifice plates with varying beta ratios, along with a 4-inch orifice plate used for testing a larger diameter.



**Figure 3.** 2-inch orifice plate's arranged as follow: the top row (left to right) contains beta ratios of 0.3, 0.4, and 0.5; the second row (left to right) contains beta ratios of 0.6, 0.7, and 0.8. The 4-inch orifice plate is positioned at the bottom.

Additionally, testing was conducted for a 2-inch butterfly valve, a 2-inch gate valve, and a 2-inch Venturi meter (Figure 4).



**Figure 4.** Tested components, including the Venturi meter (left), gate valve (middle), and the butterfly valve (right).

For the orifice plates and the Venturi meter, experiments were performed at 100%, 75%, 50%, and 25% of maximum flow rates. The butterfly valve was tested at maximum flow with openings of 90°, 60°, and 30°, while the gate valve was tested at maximum flow rates with openings of 50% and 25%. All tests were conducted under cavitation-free conditions.

Furthermore, a 4-inch orifice plate with a beta ratio of 0.5 was tested using a similar experimental setup. The downstream section of the pipe incorporated pressure taps positioned at 2D, 4D, 6D, 8D, 10D, 12D, 16D, and 20D to evaluate pressure recovery characteristics.

These devices and beta ratios were selected to represent a wide variety of flow scenarios that are encountered in the industry today. Although not all valves and meters that exist were tested, those that were tested cover a large portion of popular valves and meters used and create various types of localized disturbances that induce a high velocity jet and localized fluid acceleration. One of the key objectives was to include devices that were known flow disturbers and would present severe flow separation and turbulence through and downstream of the device.

## V. RESULTS

The results section provides an in-depth analysis of pressure recovery trends for various devices, including orifice plates, Venturi meters, butterfly valves, and gate valves. Each subsection explores experimental observations, compares them with theoretical expectations, and highlights key patterns. Graphical representations accompany the text to illustrate critical findings.

in the most noticeable pressure losses and extended recovery distances, as indicated by the steep pressure gradient observed between the 2D and 4D downstream taps. Lower flow rates showed a more gradual pressure recovery.

Figure 5 displays the pressure recovery trends for 2-inch orifice plate across various beta ratios with the upstream pressure normalized to 100 feet. To improve clarity, Figure 6 focuses exclusively on maximum flow rate conditions, showing the relationship between beta ratio and recovery distance with an experimentally-fitted hydraulic grade line (HGL). The HGL was established using friction slope data, from preliminary testing, and extended from taps located between 10D and 26D, where pressure was confirmed to be fully recovered and the flow field uniform. Experimental pressure recovery was considered complete once pressure values aligned with the slope of the experimentally determined HGL slope. Again, the pressure was normalized to 100 feet upstream for each case for ease of comparison.

Based on this analysis, pressure recovery generally occurred between 4D and 6D for the higher flow rate tests. For lower flow rates, pressure recovery generally was observed between 2D and 4D. These trends remained consistent across all beta ratios.

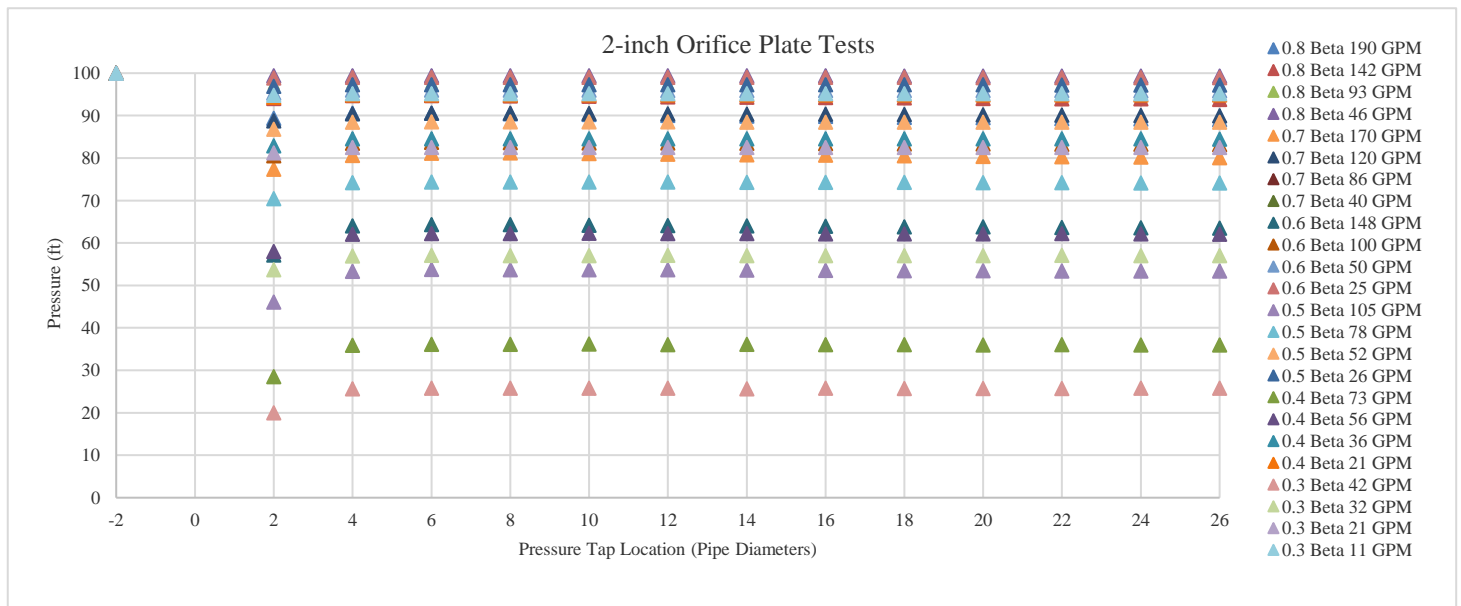


**Figure 5.** Pressure recovery trends for 2-inch orifice plates across various beta ratios.

### A. Orifice Plates

The pressure recovery trends for 2-inch orifice plates were analyzed for beta ratios ranging from 0.3 to 0.8. As expected, smaller beta ratios, such as 0.3, exhibited the highest pressure losses due to greater flow constriction and turbulence, leading to significant energy dissipation. Maximum flow rates resulted

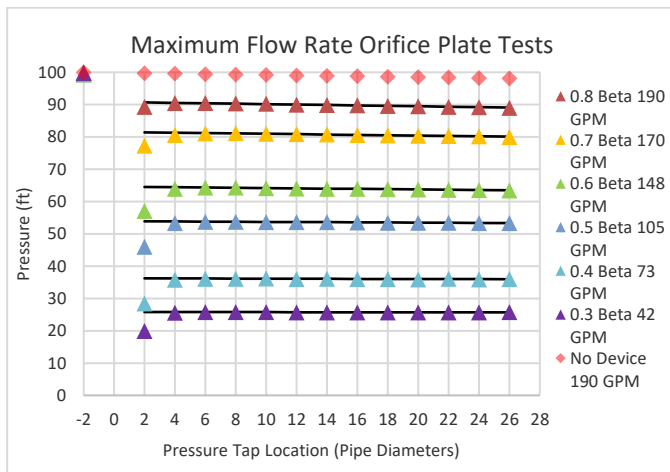


**Figure 6.** Pressure recovery trends for maximum flow rates of 2-inch orifice plates. The black lines are the experimentally fitted HGL.

### B. Venturi Meter

The Venturi meter exhibited the least permanent pressure loss among the tested devices, demonstrating highly efficient pressure recovery. The smooth transition through the Venturi minimized turbulence and energy dissipation. Figure 7 illustrates the fitted pressure recovery trends for the Venturi meter across multiple flow rates. Also shown is the HGL of the pipe in place with no device and maximum flow rate. The slope will vary with flow rate, but this allows the visualization of the amount of loss the Venturi meter causes compared to the friction loss of the pipe.

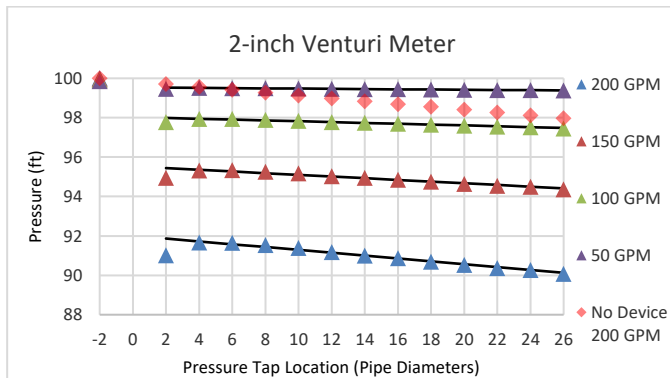


**Figure 7.** Fitted pressure recovery trends for the 2-inch Venturi meter across multiple flow rates. The black lines are the experimentally fitted HGL.

At lower flow rates, pressure returned to the HGL by 2D. As flow rates increased, pressure took slightly longer to recover, reaching equilibrium within 4D. This behavior aligns with expectations, as Venturi meters are designed to minimize head loss by gradually converging and diverging flow streams without introducing flow separation.

### C. Butterfly Valve

The butterfly valve displayed rapid pressure recovery across all tested configurations (90°, 60°, and 30° at maximum flow).

Pressure stabilized by 4D downstream for all three conditions. The 30° open condition exhibited the greatest pressure loss, causing a slightly greater deviation from the HGL at 2D. However, the recovery distance remained consistent among all tested openings. Lower flow rates were expected to recover even sooner. Figure 8 highlights the fitted pressure recovery behavior for each butterfly valve position. Also shown is the HGL of the pipe in place with no device using the maximum flow rate that was used for the 90° open test. The slope will vary with flow rate, but this allows the visualization of the amount of loss the butterfly valve causes compared to the friction loss of the pipe.

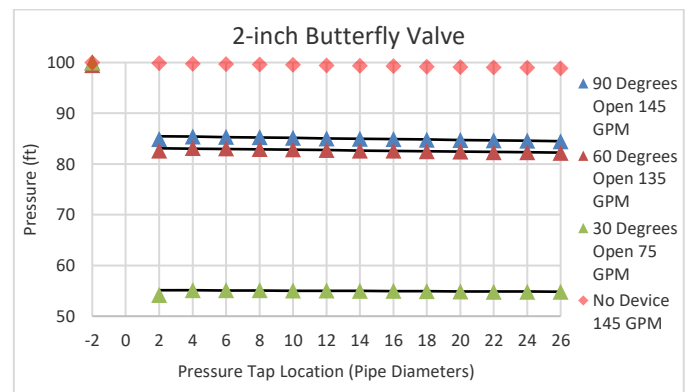


**Figure 8.** Fitted pressure recovery trend for the 2-inch butterfly valve at different open positions (90°, 60°, and 30°). The black lines are the experimentally fitted HGL.

### D. Gate Valve

Similar to the butterfly valve, the gate valve showed pressure recovery within 4D downstream. Figure 9 illustrates the fitted pressure recovery data for the gate valve. Only the 25% and 50% open conditions were tested at maximum flow, as greater openings result in minimal pressure loss. The 25% open condition exhibited greater pressure loss and a slightly longer recovery distance, but both cases demonstrated full recovery within 4D. Also shown is the HGL of the pipe in place with no device using the maximum flow rate that was used for the 50% open test. The slope will vary with flow rate, but this allows the visualization of the amount of loss the gate valve causes compared to the friction loss of the pipe.

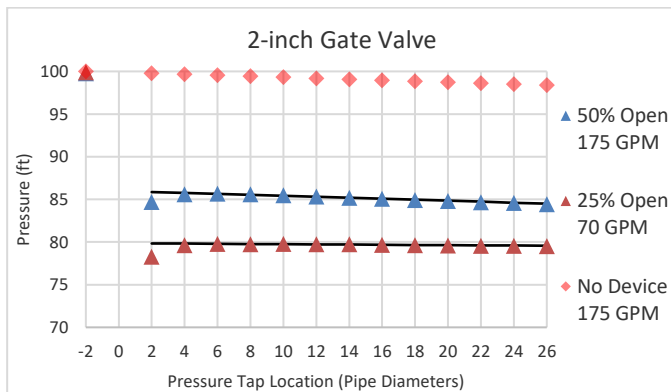


**Figure 9.** Fitted pressure recovery trend for the 2-inch gate valve at 50% and 25% open positions. The black lines are the experimentally fitted HGL.

### E. 4-inch Orifice Plate

The 4-inch orifice plate was included to verify the influence of potential size scale effects. The 4-inch 0.5 beta orifice plate followed a similar pressure recovery pattern as the 2-inch orifice plates, despite differences in test setup. Figure 10 presents the recovery trends for this configuration. Higher flow rates resulted in greater pressure loss, but pressure recovered by 4D for all flow rates. This finding contrasts slightly with the 2-inch orifice plate results, where higher flow rates extended recovery distances. It is important to note that the pressure taps for this pipe were found to be not as consistent as the 2-inch stainless steel pipe. Consequently, the pressure readings were not well behaved. Although the pressure readings show no friction loss (lack of slope in HGL readings) and the results from them should not be used for accurate HGL characterization, the overall pressure recovery trends align well with expectations can be used to assess pressure recovery.

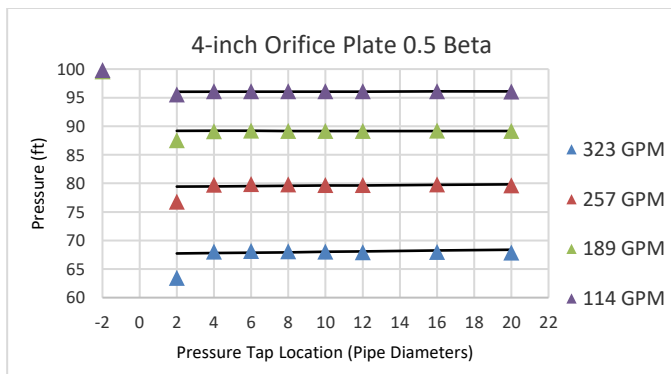


**Figure 10.** Fitted pressure recovery profile for a 4-inch orifice plate with a 0.5 beta ratio across various flow rates. The black lines are the experimentally fitted HGL.

### F. Quantitative Analysis of Pressure Recovery

To further quantify the observed trends, the percent difference between experimental and theoretical pressure recovery values were assessed, focusing on key flow rates. The theoretical pressure recovery values were obtained by the HGL

that was established using experimental friction slope data, and extended from taps located between 10D and 26D, where pressure was confirmed to be fully recovered and the flow field uniform. Table 1 presents the results for the two highest flow rates of each orifice plate configuration.

**Table 1.** Percent difference between experimentally measured and theoretically expected pressure recovery values for 2-inch and 4-inch orifice plates.

Beta Ratio	Flow (gpm)	2D	4D	6D	8D	10D
0.8	190	-1.48%	-0.04%	0.13%	0.15%	0.13%
	140	-0.77%	-0.02%	0.07%	0.08%	0.07%
0.7	170	-4.94%	-0.80%	-0.08%	0.20%	0.10%
	120	-2.11%	-0.29%	-0.04%	0.05%	0.04%
0.6	150	-11.44%	-0.68%	-0.02%	0.13%	0.01%
	100	-3.79%	-0.20%	0.06%	0.05%	0.05%
0.5	105	-14.52%	-0.92%	-0.06%	-0.07%	-0.06%
	78	-5.42%	-0.28%	-0.02%	0.00%	0.01%
0.4	73	-21.37%	-0.97%	-0.13%	-0.11%	0.16%
	55	-6.93%	-0.31%	-0.04%	-0.02%	0.06%
0.3	42	-22.58%	-0.66%	0.02%	0.06%	0.09%
	32	-5.94%	-0.23%	0.00%	-0.03%	-0.10%
4-inch 0.5 Beta	323	-6.38%	0.33%	0.43%	0.22%	-0.01%
	257	-3.33%	0.31%	0.40%	0.29%	0.12%

According to the ANSI/ISA S75 standard [1] and American Water Works Association (AWWA) Manual of Water Supply Practices: Quarter-Turn Valves: Head Loss, Torque, and Cavitation Analysis [11], the accuracy of differential pressure measurements must remain within an error range of  $\pm 2\%$  of the measured pressure differential. Given these standards, the authors sought to refine the accuracy even further, opting for a stricter  $\pm 0.5\%$  threshold. This decision was made to enhance confidence in the author's assessments, ensuring that pressure recovery distances were evaluated with higher precision than typically required by industry standards.

Using this refined error margin, pressure recovery was observed within 6D for all beta ratios except 0.8, which recovered within 4D. If the standard  $\pm 2\%$  error range were used, all orifice plates would appear to recover within 4D, with some even stabilizing by 2D. The stricter  $\pm 0.5\%$  threshold provides greater confidence in these findings.

Table 2 presents similar analyses for the butterfly valve, gate valve, and venturi meter. Results indicate that pressure recovery occurred by 4D for all devices under the  $\pm 0.5\%$  error threshold. If a  $\pm 2\%$  error range were applied, all devices would show recovery by 2D. These findings suggest that shorter measurement distances may be sufficient in some applications.

**Table 2.** Percent difference between experimental and theoretical pressure recovery values for butterfly valves, gate valves, and the Venturi meter.

Device Type	Flow Condition	2D	4D	6D	8D	10D
Butterfly Valve	90° Open	-0.66%	0.03%	0.09%	0.07%	0.06%
	60° Open	-0.53%	0.12%	0.15%	0.11%	0.08%
	30° Open	-1.66%	0.02%	0.12%	0.14%	0.09%
Gate Valve	50% Open	-1.32%	-0.15%	0.06%	0.09%	0.10%
	25% Open	-1.93%	-0.23%	-0.01%	0.01%	0.04%
Venturi Meter	200 GPM	-0.93%	-0.06%	0.09%	0.11%	0.11%
	150 GPM	-0.51%	-0.03%	0.06%	0.08%	0.08%

**G. Permanent Pressure Loss versus Loss Associated with  $C_v$  Value**

When analyzing pressure losses across control valves and flow meters, it is important to differentiate between total pressure drop ( $\Delta P$ ), permanent pressure loss ( $PL$ ), and the pressure loss associated with the  $C_v$  value. The flow coefficient,  $C_v$ , is commonly used to characterize a valve's ability to pass flow under a given pressure drop. However,  $C_v$  alone does not indicate how much of the pressure drop is recovered downstream versus how much is permanently lost due to turbulence, separation, and energy dissipation.

To assess the proportion of the pressure loss that remains unrecovered, the permanent pressure loss ratio is defined as Eq. 7.

$$\frac{PL}{\Delta H} = \frac{\text{Pipe HGL} - \text{Device HGL}}{\text{Pressure drop measured between 2D upstream and 6D downstream}} \quad (7)$$

This ratio provides insight into the fraction of pressure loss associated with the flow coefficient that is irreversible, distinguishing recoverable losses from permanent losses.

The results confirm that as the beta ratio decreases, the permanent pressure loss ratio increases, as shown in Table 3. Smaller beta ratios create greater flow constriction and turbulence, leading to higher energy dissipation and reduced pressure recovery.

**Table 3.** Permanent pressure loss ( $PL/\Delta H$ ) for orifice plates.

Orifice Plate Beta Ratio	Average Permanent Loss Ratio ( $PL/\Delta H$ )
0.8	0.940
0.7	0.970
0.6	0.990
0.5	0.995
0.4	0.997
0.3	0.998

Higher beta ratios (e.g., 0.8) exhibit some degree of pressure recovery, while lower beta ratios (e.g., 0.3) show nearly 100% permanent loss. The sharp contraction and increased turbulence at smaller beta ratios result in almost complete energy dissipation, meaning that the pressure drop measured across the orifice plate closely represents actual system losses.

Unlike orifice plates, the Venturi meter, butterfly valve, and gate valve exhibit varying degrees of pressure recovery, leading to different permanent loss ratios. The Venturi meter, designed for efficient flow transitions, minimizes turbulence and recovers a significant portion of its pressure loss. In contrast, throttling valves (such as butterfly and gate valves) generate turbulence and flow separation, leading to greater pressure losses.

Table 4 presents the permanent loss percentages for these devices under different operating conditions. The results show that the Venturi meter consistently exhibits the lowest permanent loss percentages, while the butterfly and gate valves experiences higher irreversible energy losses, especially at more restrictive positions.

**Table 4.** Permanent pressure loss ( $PL/\Delta H$ ) for a butterfly valve, gate valve, and a Venturi meter.

Device Type	Flow Condition	Permanent Loss Ratio ( $PL/\Delta H$ )
Butterfly Valve	90° Open	0.981
	60° Open	0.989
	30° Open	0.999
Gate Valve	50% Open	0.968
	25% Open	0.995
Venturi Meter	200 GPM	0.922
	150 GPM	0.919
	100 GPM	0.909
	50 GPM	0.875
	25 GPM	0.846

The Venturi meter exhibits the best pressure recovery characteristics, with permanent loss ratios decreasing as flow rates decrease (e.g., 0.922 at 200 gpm to 0.846 at 25 gpm). This confirms that gradual flow transitions significantly reduce energy dissipation compared to devices with abrupt flow restrictions.

In contrast, throttling valves exhibit higher permanent pressure losses, particularly at more closed positions. The butterfly valve at 30° open experiences nearly 100% permanent loss (99.9%), confirming that at restrictive positions, flow separation and turbulence cause almost complete energy dissipation. The gate valve follows a similar trend, with the 25% open condition exhibiting 99.5% permanent loss.



**H. Comparison of Permanent Pressure Loss Ratio to the Loss Coefficient (K)**

To further analyze energy dissipation in flow systems, the relationship between the permanent pressure loss ratio ( $PL/\Delta H$ ) and the loss coefficient ( $K$ ) was examined. The loss coefficient,  $K$ , quantifies the resistance a device imposes on the flow due to turbulence, separation, and geometric restrictions. Since higher loss coefficients correspond to increased energy dissipation, a strong correlation between  $PL/\Delta H$  and  $K$  was expected. The familiar equation for the loss coefficient,  $K$ , is given by Eq. 8.

$$K = \frac{2g\Delta H}{V^2} \tag{8}$$

Where  $g$  is the acceleration of gravity,  $\Delta H$  is the head loss of the device and  $V$  is the average velocity.

Figure 11 illustrates the relationship between permanent pressure loss and the loss coefficient, with the x-axis presented on a logarithmic scale to accommodate the broad range of  $K$  values across different devices.

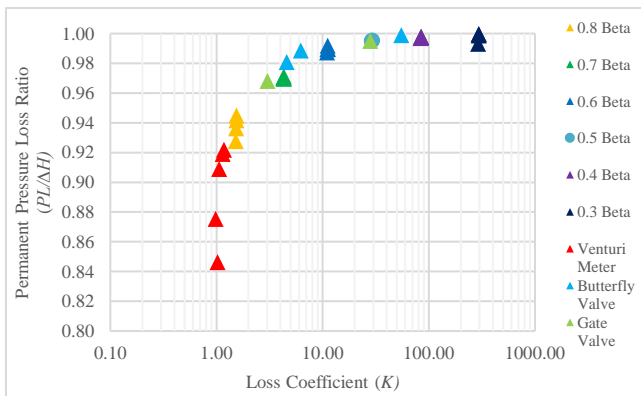


**Figure 11.** Relationship between permanent pressure loss ratio ( $PL/\Delta H$ ) and the loss coefficient ( $K$ ). The x-axis is presented on a logarithmic scale to better illustrate the relationship across different magnitudes of loss coefficients.

The data confirms a clear trend: devices with higher loss coefficients recover a greater portion of the permanent loss measured across the device than do those devices with a lower loss coefficient. This finding reinforces that restrictive geometries, such as those found in orifice plates and partially closed valves, induce significant turbulence and energy dissipation, resulting in unrecoverable pressure loss nearer to the device inducing the loss while those with lower loss coefficients continue to recover pressure downstream of the measurement location. The extent of the variation of the losses relative to the device inducing the losses, should be evaluated on a case-by-case basis for assessment of overall system head loss performance.

**VI. DISCUSSION**

The results of this study provide valuable insights into pressure recovery trends for various flow restrictions and their implications for hydraulic system design. By analyzing the relationship between pressure loss and pressure recovery distances, this study builds upon existing research and refines conventional engineering assumptions regarding pressure recovery in closed conduit systems.

Comparing these findings with previous research, such as Tullis [2] and Rahmeyer [5], confirms that pressure recovery distances of 5D-10D are generally valid, however this study demonstrates that pressure is well-recovered by 6D and, in many cases, within 4D. Recordings closer than 4D result in pressure differentials that are larger than the actual while going beyond 6D begins to include pipe loss which would then be attributed to the device.

Furthermore, the findings confirm that the industry standard of placing pressure taps 2D upstream and 6D downstream, as recommended by the ISA 75.02 standard [1], is sufficient for accurate pressure recovery assessment. The data strongly support this guideline, reinforcing its applicability across various valve types and flow conditions. Based on the results, the authors agree with the ISA standard that these recommended distances adequately capture recovered pressure with minimizing measurement errors.

Devices with smoother internal transitions, such as the Venturi meter, show significantly faster pressure recovery, likely due to reduced turbulence and energy dissipation compared to orifice plates. Unlike Rahmeyer [5], who suggested a minimum of 8D for complete recovery in butterfly valves, the results of this study show stabilization within 4D. These findings suggest that shorter measurement distances may be sufficient for practical applications, potentially leading to more compact system designs and reduced material costs.

The results also highlight the difference between  $C_v$ -based pressure loss and permanent pressure loss, emphasizing that  $C_v$  alone does not indicate how much pressure is permanently lost versus what is recovered downstream. While  $C_v$  provides a useful metric for estimating pressure drop across a valve, it does not differentiate between recoverable pressure loss due to flow separation and permanent losses caused by turbulence and energy dissipation.

Pressure recovery varies by device, with the Venturi meter exhibiting the highest recovery. Permanent loss percentages decrease at lower flow rates, further demonstrating that smooth flow transitions minimize energy dissipation. In contrast, throttling valves such as butterfly and gate valves exhibit significantly higher permanent losses, particularly at more restrictive positions. The butterfly valve at 30° open experiences nearly 100% permanent loss (99.9%), and the gate valve at 25% open exhibits 99.5% permanent loss, confirming that flow-separating devices induce significant turbulence. Similarly, orifice plates with low beta ratios exhibit near-total

energy dissipation, making their measured pressure drop closely represent the actual system energy loss.

It is important to recognize that  $C_v$ -based pressure loss is not necessarily the same as permanent pressure loss. Engineers designing flow systems should be aware that over-reliance on  $C_v$  values alone can lead to misjudging energy efficiency and pressure recovery behavior. While a high  $C_v$  value may suggest low resistance, it does not indicate whether lost pressure will recover downstream or be permanently dissipated. This distinction is critical for optimizing flow measurement placement and ensuring accurate pipeline performance calculations.

Additionally, the results show a strong correlation between the permanent pressure loss ratio ( $PL/\Delta H$ ) and the loss coefficient ( $K$ ), suggesting that  $K$  can serve as a practical predictor of permanent pressure loss when direct pressure recovery measurements are unavailable. However, it is important to recognize that while  $K$  provides a standardized method for estimating energy losses, it does not inherently distinguish between recoverable and permanent losses. While  $K$  provides a useful estimate of energy losses, it does not account for pressure recovery. Engineers should use it in combination with direct pressure recovery measurements to ensure accurate system efficiency evaluations.

This study further highlights that orifice plates, throttling valves, and other restrictive devices with higher  $K$  values exhibit greater permanent pressure loss, meaning that the pressure drop measured across these devices using 2D and 6D pressure taps closely represents actual system energy loss. In contrast, the Venturi meter and other streamlined components recover a greater percentage of the pressure loss than that measured at 2D and 6D pressure taps due to their design, which minimizes turbulence and separation. These findings reinforce the importance of considering both  $K$  and pressure recovery trends when evaluating system efficiency and optimizing flow control devices.

The implications of these findings extend to practical pipeline design and system efficiency. Recognizing device-specific pressure loss characteristics allows engineers to improve system layouts, reducing both material cost and energy losses. By considering both pressure recovery distances and permanent pressure losses, engineers can more accurately model system performance, optimize pipeline efficiency, and ensure precise flow control in fluid transport applications.

## VII. CONCLUSIONS

This study experimentally investigated pressure recovery distances downstream of various hydraulic disturbances, including orifice plates, a Venturi meter, a butterfly valve, and a gate valve, across multiple flow conditions. The findings confirm that pressure recovery generally occurs between 4D and 6D downstream of the disturbance, with variations depending on the device type and flow characteristics. While industry standards (ANSI/ISA-75.02) recommend a 6D

placement for downstream pressure taps, this research shows that, in many cases, pressure stabilizes within 4D, and extending beyond 6D can incorporate pipe friction losses rather than actual device-induced pressure loss.

The Venturi meter exhibited the fastest pressure recovery, with stabilization occurring as early as 2D to 4D, highlighting its efficiency in minimizing turbulence and energy dissipation. In contrast, orifice plates with lower beta ratios (0.3 to 0.5) exhibited longer recovery distances and nearly 100% permanent pressure loss, confirming their role as significant energy dissipaters. Throttling valves, such as butterfly and gate valves, showed pressure recovery within 4D; however, at more restrictive positions (e.g., butterfly valve at 30° open and gate valve at 25% open), nearly all the pressure loss was permanent.

A key distinction identified in this study is the difference between  $C_v$ -based pressure loss and permanent pressure loss. While  $C_v$  is commonly used to estimate flow behavior, it does not differentiate between recoverable and permanent losses. The results show that devices with high loss coefficients ( $K$ ) experience a greater permanent pressure loss ratio, whereas those with lower  $K$  values, such as the Venturi meter, have a smaller permanent pressure loss ratio. The strong correlation between permanent pressure loss ( $PL/\Delta H$ ) and  $K$  suggests that  $K$  can be a useful predictor of how much pressure losses is likely to be permanent versus recoverable, especially when direct measurements are unavailable and the flow coefficient of the device is available.

By providing a detailed analysis of pressure recovery trends and distinguishing between recoverable and permanent pressure losses, this study refines existing engineering assumptions and supports the validity of the 6D standard placement for pressure taps. These findings have practical implications for optimizing measurement placement, improving pipeline efficiency, and ensuring accurate pressure loss assessments in hydraulic system design. Future research should further explore pressure recovery behavior in larger diameter pipes and under varying turbulence conditions to refine industry standards further.

## REFERENCES

- [1] ANSI/ISA, 1996. ANSI/ISA-75.02-1996, *Control Valve Capacity Test Procedures*.
- [2] Tullis, J. P. 1989. *Hydraulics of Pipelines: Pumps, Valves, Cavitation, Transients*, A Wiley-Interscience Publication
- [3] ISO (2008). ISO 9644:2008, *Agricultural irrigation equipment-Pressure losses in irrigation valve-Test method*.
- [4] Manserat, J., A. Rubio, L.O. Cots, 2019. "Diaphragm Valve Hydraulic Behavior Depending on Operating Pressure." *Journal of Irrigation and Drainage Engineering* Nov 2019, 145 (11)
- [5] Rahmeyer, W., L. Driskell, 1985. "Control Valve Flow Coefficients." *Journal of Transportation Engineering* 111 (4) 358-364.
- [6] Ball, J. W. 1957. "Cavitation Characteristics of Gate Valves and Globe Valves Used as Flow Regulators Under Heads Up to About 125 Feet." *Trans. ASME*. Aug 1957, 79(6) 1275-1281.
- [7] Huang, C., R. H. Kim, 1996. "Three-Dimensional Analysis of Partially Open Butterfly Valve Flows." *J. Fluids Eng.* Sep 1996, 118(3) 562-568.

- [8] Pradeep, A. G., G. G. Gorantla, V. Turaga, V. Srinivasa. 2022. "A Study on Improving the Flow Capacity of the Valves." *International Scholarly and Scientific Research & Innovation* 16(11).
- [9] Thapa, P. B. 2016. "Flow Measurement and Control system in oil gas industry." Unpublished Internal Report, Dec 2016.
- [10] Nguyen, Q. K., K. H. Jung, G. N. Lee, S. B. Suh, P. To, 2020. "Experimental Study on Pressure Distribution and Flow Coefficient of Globe Valve." *Processes* 2020, 8(7) 875.
- [11] Bosserman, B. E., J. R. Holsterom, 2017. *Quarter-Turn Valves: Head Loss, Torque, and Cavitation Analysis*. Edited by American Water Works Association. Third Editions.